Core-state manipulation of single Fe impurities in GaAs with a scanning tunneling microscope

J. Bocquel,[1] V. R. Kortan,[2] C. Şahin,[2] R. P. Campion,[3] B. L. Gallagher,[3] M. E. Flatté,[1,2] and P. M. Koenraad[1]

[1]*Department of Applied Physics, Eindhoven University of Technology, P.O. Box 513, 5600 MB, Eindhoven, The Netherlands*

[2]*Optical Science and Technology Center and Department of Physics and Astronomy, University of Iowa, Iowa City, Iowa 52242, USA*

[3]*School of Physics and Astronomy, University of Nottingham, Nottingham NG7 2RD, United Kingdom*

(Received 29 February 2012; published 14 February 2013)

We demonstrate that a scanning tunneling microscope tip can be used to manipulate the tightly bound core (d-electron) state of single Fe ions embedded in GaAs. Increasing tip-sample voltage removes one d electron from the core of a single Fe, changing the dopant from the $(Fe^{2+})^-$ ionized acceptor state to the $(Fe^{3+})^0$ isoelectronic state, which alters the spin moment and dramatically modifies the measured local electronic contrast in topographic maps of the surface. Evidence of internal transitions among the d states of the Fe core is also seen in topographic maps where dark anisotropic features emerge from the interference between two paths: the direct tip-sample tunneling and tunneling which excites a d-state core exciton of the Fe dopant.

DOI: 10.1103/PhysRevB.87.075421 PACS number(s): 73.20.Hb, 68.37.Ef

I. INTRODUCTION

Control and measurement of the electronic, magnetic, and optical properties of a single electronic state in a semiconductor has advanced rapidly over the past several years[1] and is approaching the point of significant technological importance.[2–5] Achievements include controlled positioning of small numbers of dopants within the semiconducting host,[4,6–9] with quantitative theoretical descriptions of their wave functions,[10,11] as well as local perturbations of their properties including optical orientation of their spin,[12] electrical control of their charge state,[13,14] and electrical probing of their spin excitations.[15] Electronic manipulation of dopant charge states has been predominately limited to ionization of Coulombically bound (shallow) donor and acceptor levels,[14,16] although switching a Si dopant between a substitutional and interstitial position with an associated charge change has also been demonstrated.[17] Electronic manipulation of tightly bound states, especially the spin-polarized core d electrons of transition-metal dopants, would permit a wider range of novel phenomena, including changing the core spin and magnetic interactions of a dopant. Such transitions have been measured optically for ensembles of transition-metal dopants in semiconductors,[18] and there is evidence of multiple d states associated with single transition-metal dopants embedded in the surface layer.[19] Direct electrical manipulation of the charging of these core states, however, has not been demonstrated, especially for a single dopant that is tetrahedrally bonded with the host and hence has the symmetry of a bulk substitutional site.

Here we directly demonstrate the electrical manipulation of the core electronic state of a single substitutional Fe atom deeply embedded within GaAs using a scanning tunneling microscope tip. We directly observe the different charge and valence states of Fe on the atomic scale using cross-sectional scanning tunneling microscopy (X-STM) and remove a d electron from the core by increasing the tip voltage, causing the transition from the $3d^6$, ionized acceptor configuration $(Fe^{2+})^-$ to the $3d^5$, isoelectronic state $(Fe^{3+})^0$ of iron. This manipulation differs from shallow-state ionization of dopants, such as the ionization of a Mn acceptor in GaAs (Ref. 13), because of this change in d-state occupation. We note the $3d^6$ $(Fe^{2+})^-$ acceptor state of an Fe atom in the top layer of a p-type GaAs surface has been observed, but the charge state was not demonstrated to be manipulated.[19] We also find evidence of the internal transitions of the d states in the core, through identification of anisotropic dark features in the topography, which are associated with the interference of a tunneling path that excites a d-state core exciton with the tunneling path corresponding to direct tunneling from the tip to the sample. The spatial range and dark character of the feature are consistent with our calculations.

The known possible electronic configurations of an Fe atom in GaAs[20] are illustrated in Fig. 1. Like most $3d$ transition metals, Fe impurities in III-V semiconductors act as charge traps and recombination centers, pinning the Fermi level at a deep energy level and inducing semi-insulating properties within the host. An I(V) curve acquired on the clean GaAs surface in the Fe-doped region of the investigated sample is displayed in Fig. 2.

These deep levels, called charge-transfer (CT) levels, correspond to a change in the valence state of the Fe atom and are expected to have a localized atomiclike character. The stable electronic configuration is determined by the position of the Fermi level in the semiconductor relative to the CT levels. Thus, in GaAs, when substituting for the Ga cation site, an Fe atom can be in two different valence states: Fe^{3+} or Fe^{2+}. Fe^{3+} has a half-filled d shell and acts as an isoelectronic impurity, whereas Fe^{2+} with six electrons in the d shell acts as an acceptor. Fe will be in its acceptor state or in its isoelectronic state depending on whether the Fermi level is found above or below the Fe^{2+}/Fe^{3+} CT level which is located 510 meV above the valence band edge.[20] Moreover, Fe in its acceptor state Fe^{2+} can be in two different charge states, A^0 or A^-, where A^- corresponds to the ionized acceptor $(Fe^{2+})^-$ and A^0 to the neutral acceptor state $[Fe^{2+}, h^+]^0$. This neutral state, consisting of a hole bound to the ionized acceptor $(Fe^{2+})^-$ carrying a single negative charge,[20,21] is expected to have a delocalized, hostlike character. The ionization energy associated with these charge states, i.e., the energy needed for $(Fe^{2+})^-$ to bind a free hole and form the $[Fe^{2+}, h^+]^0$ complex, is 25 meV. To summarize, the three electronic configurations reported for Fe impurities in GaAs and described in Fig. 1 can be denoted by the following: $(Fe^{3+})^0$, $(Fe^{2+})^-$, and $[Fe^{2+}, h^+]^0$.

 ©2013 American Physical Society

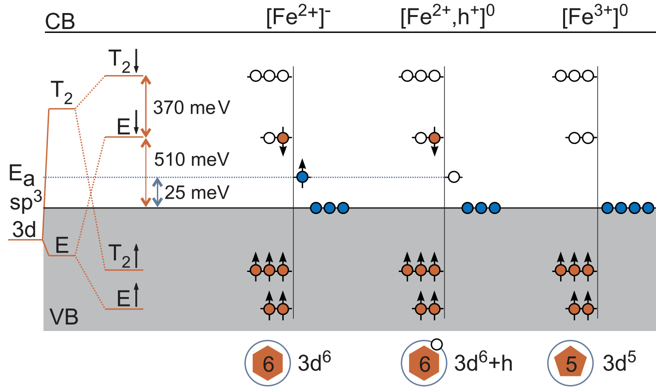

FIG. 1. (Color online) Possible electronic configurations of an Fe atom in GaAs. The $3d$ electrons of Fe populate core levels (orange), as well as delocalized anti-bonding states (blue) arising from their hybridization with As neighbors. The charge transfer level from Fe^{2+} (5 d-electrons) to Fe^{3+} (6 d-electrons) corresponds to a localized energy level found 510 meV above the VB edge. The energy level associated with the bound hole state $(Fe^{2+})^- + h^+$ is found 25 meV above the VB edge. The most stable configuration is determined by the position of the Fermi level relative to these energy levels.

II. EXPERIMENT

The presented data are the result of different X-STM measurements performed both at room temperature and 77 K under UHV conditions (5×10^{-11} Torr). Several electrochemically etched tungsten STM tips were used. The STM was operated in constant current mode on a clean and atomically flat GaAs (110) surface obtained by *in situ* cleavage. The molecular beam epitaxy grown sample contains a 100-nm Fe-doped GaAs layer (nominal concentration of 2×10^{18} cm^{-3}) and a Fe monolayer incorporated in GaAs. The growth temperature was 580 °C during the entire growth procedure. The nominal layer structure consisted of GaAs substrate/100 nm Fe:GaAs/200 nm GaAs/Fe monolayer/500 nm GaAs. The growth was monitored by RHEED. As expected for transition

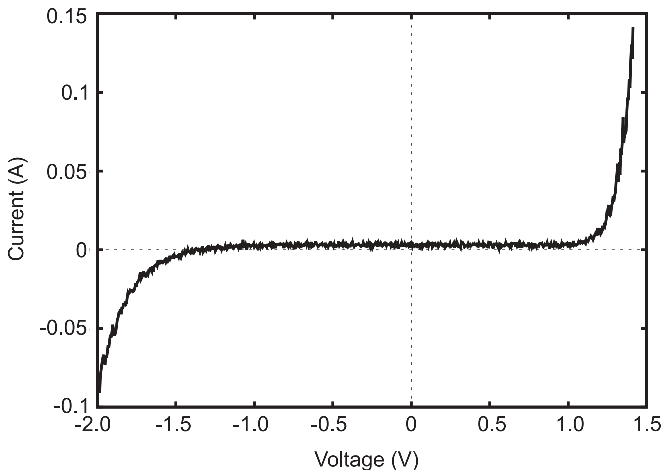

FIG. 2. I(V) curve acquired on the clean GaAs surface in the Fe-doped region. This plot is consistent with the Fe doping (5×10^{17} cm^{-3} in this area) of the otherwise intrinsically doped GaAs. The sample Fermi level is found deep in the band gap. The shift of the I(V) curve from 0 is a known effect of the I-V converter.

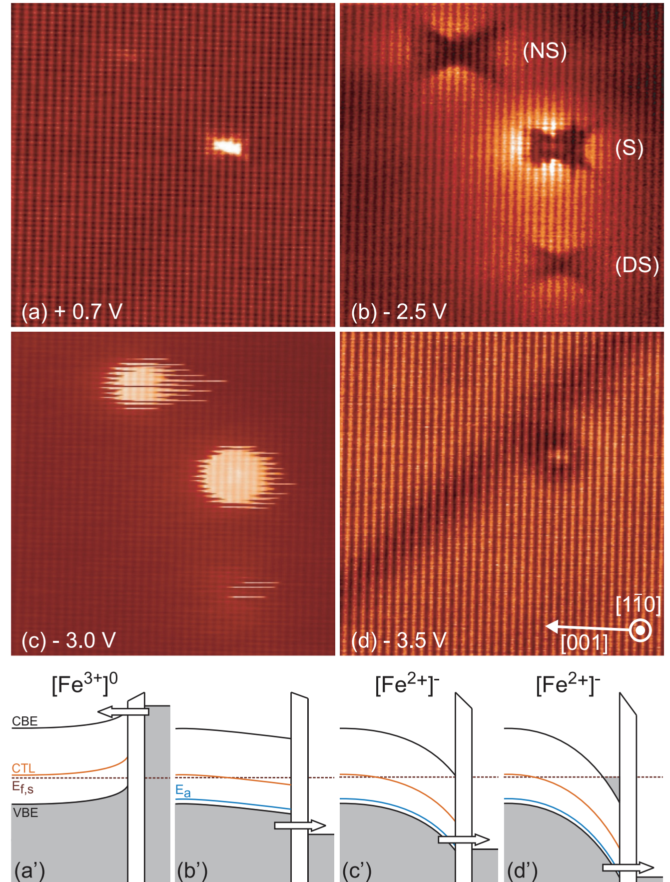

FIG. 3. (Color online) (a)–(d) 23 × 23-nm topography images of single Fe impurities in GaAs taken at the same position but different voltages. Bringing the W tip close to the sample surface induces a bending of the semiconductor bands and shifts the associated energy levels as seen in the corresponding band diagrams (a′)–(d′). Thus, changing the voltage between tip and sample locally changes the Fermi level and brings the Fe impurities into different electronic states. (a) isoelectronic acceptor Fe^{3+}. (b),(c) Ionized acceptor $(Fe^{2+})^-$. (d) Ionized acceptor $(Fe^{2+})^-$ screened by an accumulation of electrons at the surface. The Fe impurities are located at different positions from the cleaved surface: in the surface layer (S), near the surface (NS), and deep below the surface (DS).

metals in III-V semiconductors,[22] the Fe atoms in our sample strongly segregate along the growth direction. The concentration of Fe in the region where the STM measurements were performed is 5×10^{17} cm^{-3}, as determined by Secondary Ion Mass Spectrometry (SIMS). The details of the incorporation of Fe in GaAs are reported elsewhere.[23]

This dilute distribution allowed us to probe single Fe atoms and determine the local electronic contrast induced by each impurity. Figure 3 shows constant current filled states topography taken at different voltages at a position where three Fe atoms are visible. The local electronic contrast induced by each Fe impurity is strongly dependent on the applied voltage. We distinguish four regimes for which Fe atoms give rise to images with distinctly different contrasts and shapes, caused by local manipulation of the Fermi level position from tip-induced band bending (TIBB) due to the applied voltage. The Fermi level position within the band gap controls the electronic

configuration of Fe atoms in the semiconductor. Thus, tuning the voltage is expected to change the charge state and/or the valence of the impurities as described in Fig. 3. Impurity charge manipulation using an STM tip or a nearby charged defect has already been demonstrated for various impurities in III-V semiconductors;[9,14,16] however, a change of the d-state core occupation has not been observed before.

III. RESULTS AND DISCUSSIONS

At positive voltage, some Fe atoms appear as bright localized features, even though the majority are not visible. Locally under the tip the semiconductor's bands as well as the CT level are pushed upwards and the sample Fermi level will be located below the Fe^{2+}/Fe^{3+} CT level. Under these conditions the Fe atoms are expected to be in their isoelectronic configuration Fe^{3+}. The contrast observed for isoelectronic Fe atoms originates from the difference in local density of states (LDOS) of the Fe atoms and the Ga atoms. This should give rise to such a localized contrast that only impurities located in the surface layer (S) are expected to appear in the STM images. The contrast shown in Fig. 3(a) is therefore consistent with Fe atoms in the Fe^{3+} configuration. The slightly delocalized features can be understood as a consequence of a hybridization of Fe with the valence band wave functions. The absence of electronic contrast for the large majority of the Fe impurities at positive applied voltage is better shown in Fig. 4. From these observations we can confirm that at positive voltage Fe atoms are in their isoelectronic configuration Fe^{3+}.

Figure 3(c) shows that for an applied voltage of ≈ -3.0 V the Fe atoms appear as bright disks. Such disks are associated with the ionization of either donors[14] or acceptors.[9] In these studies, the onset of the disk indicates the spatial separation between the tip and the impurity resulting in a local TIBB sufficient to ionize the neutral impurity. The isotropic Coulomb field created by an ionized impurity induces a local enhancement of the states available for tunneling and thus the tunnel current. For tunneling conditions like Fig. 3(c), the Fe impurities are in their isoelectronic configuration when the tip is far away. However, at negative voltage locally under the tip, the bands and energy levels are bent downwards. Thus, as the tip is brought closer to the impurity, the Fe^{2+}/Fe^{3+}CT level crosses the semiconductor Fermi level and the most favorable valence state for Fe switches from Fe^{3+} to $(Fe^{2+})^-$. This mechanism, illustrated in Fig. 5, is consistent with the increasing disk diameter found with increasing applied voltage. Taken note of the change the Fe impurities release a core d-state hole, whereas former studies on Mn acceptors and Si donors report, respectively, on the loss of a bound valence hole or a bound conduction electron. Here the neutral state is Fe^{3+}, not the effective-mass-like complex $[Fe^{2+},h^+]^0$. The filling of the 3d-shell changes from five to six electrons, and therefore the core spin state changes from $S = 5/2$ to $S = 2$. The presence of these bright disks in our topography images is a clear manifestation of the manipulation of the d states of single Fe impurities by the STM tip.

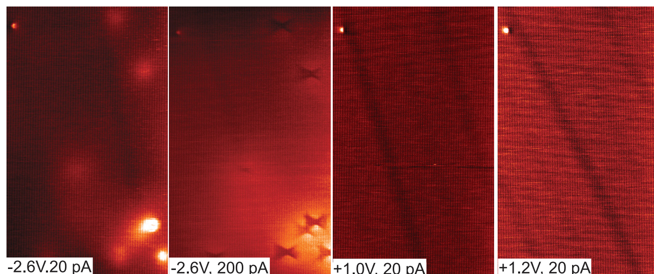

FIG. 4. (Color online) 30 × 50-nm topography images of Fe impurities in GaAs taken at different voltages. At negative voltage the Fe impurities give rise to different electronic contrasts. The absence of electronic contrast at positive voltage is attributed to the position of the impurities below the surface.

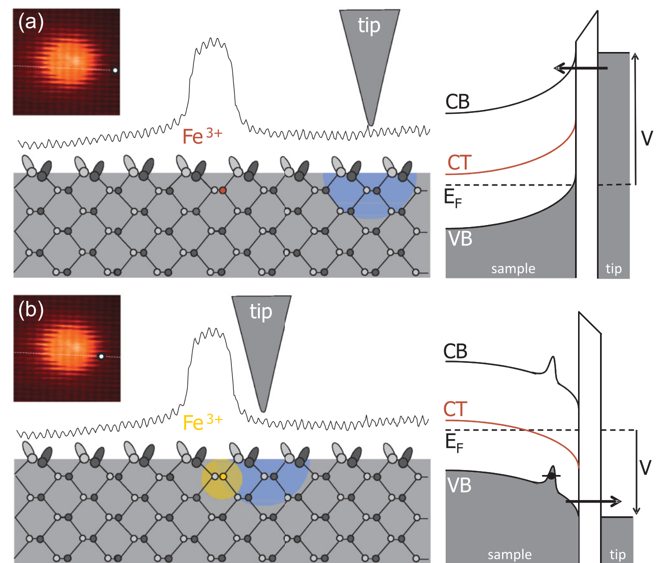

FIG. 5. (Color online) Illustration of the ionization mechanism, displaying the height profile across the disk. (a) The tip is far from the Fe impurity, in its Fe^{3+} state. (b) The tip is close enough to the Fe impurity to bring it in its $(Fe^{2+})^-$. The band diagrams indicate the position of the Fe^{2+}/Fe^{3+}CT level relative to the sample Fermi level. (Insets) 10 × 10-nm filled state topography image of a single Fe impurity in GaAs taken at -3.0 V. The disk is induced by the presence of an isotropic Coulomb field around the $(Fe^{2+})^-$ ionized impurity.

Figure 3(d) shows the electronic contrast appearing for Fe atoms at very large negative voltage. In this case, the semiconductor's bands are bent further downwards such that an accumulation of electrons is created at the surface of the semiconductor. These electrons screen charged defects and lead to charge density oscillations around each negatively charged $(Fe^{2+})^-$ ion. The presence of such Friedel-like oscillations has already been reported for ionized dopants in n-type semiconductors such as Si (Ref. 24) and Mn (Ref. 25) in GaAs. This observation requires a sample Fermi level relatively high in the band gap; in our Fe-doped GaAs sample, the Fermi level is close to the CT level, located deep in the band gap, but is shifted much higher, near the surface and at these voltages, by the TIBB.

Having described the features associated with changing the charge state of the Fe by the tip, we now discuss the peculiar features of the electronic contrast in the topography for a single

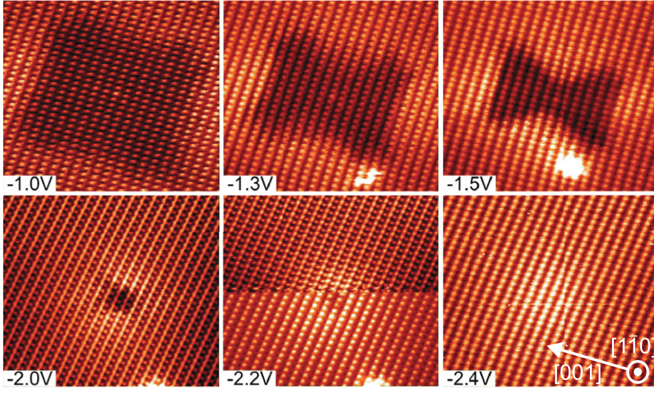

FIG. 6. (Color online) 12 × 14-nm filled states topography images of the same Fe impurity deep below the surface in GaAs, taken at different negative voltages. The dark feature corresponds to a decrease in conductivity. The shape becomes smaller and more asymmetric as the TIBB becomes larger.

Fe atom at low negative bias voltage [Fig. 3(b)], in which all Fe atoms appear as dark anisotropic features on a brighter background. The shape of this feature for a single impurity is very sensitive to the applied voltage and the current set point, and its voltage dependence is shown in Fig. 6. From very low to moderate negative voltage, the lateral extension of this dark feature decreases and becomes more asymmetric before disappearing. The same dependence is found when decreasing the current set point.

Similar anisotropic shapes, but with bright contrast, have been reported for the wave functions of holes bound to individual acceptors in GaAs (Refs. 13, 19, and 26). Bound hole wave functions are imaged at low positive voltage, when electrons can tunnel from the tip to the empty acceptor state and appear as bright anisotropic features. There the anisotropy of the contrast originates from the cubic symmetry of the host crystal,[13] and the asymmetry is related to the interaction with the surface and the binding energy of the acceptor.[27] Thus, the shape variation of these features from one Fe atom to the other is attributed to the depth dependence of the charge distribution contrast, as shown for Mn impurities in GaAs.[28] The voltage dependence is understood as a consequence of the TIBB. The shapes become smaller and more asymmetric as the TIBB becomes larger. The current dependence however, is weaker and cannot be understood as a result of a change in TIBB. The asymmetry of the shape of the measured contrast becomes stronger when the current set point decreases, i.e., when the tip-sample distance is large and the TIBB smaller. This suggests an influence of the overlap between tip and sample wave functions on the anisotropy of this electronic contrast.

IV. THEORETICAL FRAMEWORK

Decreases in conductivity appearing at a single impurity in filled states topography images are rare and only a few electron tunneling mechanisms have been reported that can account for it. The contribution to the tunneling current of an inelastic tunneling path is small and positive. However, within the framework of inelastic electron tunneling spectroscopy, for single magnetic adsorbates[29] or single molecules[30] on a metallic surface, decreases in tunneling current have been observed. In the case of a magnetic atom, the LDOS directly above the impurity can be reduced by tunneling through the Kondo resonance that develops due to the screening of the moment localized on the magnetic adatom. The phenomenon we observe is particularly robust (present at room temperature) so Kondo-like resonances in our system are unlikely.

Instead, our interpretation draws on observations of a decrease in tunneling current due to interference between two elastic tunneling paths through a single molecule, one path virtually exciting a vibrational resonance.[31–34] Here we consider a similar scenario with two distinct elastic paths from the tip to the sample: one passing directly through without disturbing the Fe impurity core electrons and one virtually exciting an electronic transition from the E to the T_2 crystal-field-split states in the d shell. In this case and using similar formalism as Ref. 31, the contribution of the second elastic path that virtually excites the core exciton, $\partial I/\partial V$, normalized to the path that does not excite the core exciton, can be written as in Ref. 31:

$$\frac{\partial I}{\partial V} = \frac{\delta\epsilon^2}{(E_a - E_{f,s})^2 + (\Gamma/2)^2} \times \left[\frac{(E_a - E_{f,s} + \omega)^2 - (\Gamma/2)^2}{(E_a - E_{f,s} + \omega)^2 + (\Gamma/2)^2} \Theta(V + \omega) + \frac{1}{\pi} \frac{(E_a - E_{f,s} + \omega)\Gamma}{(E_a - E_{f,s} + \omega)^2 + (\Gamma/2)^2} \ln\left|\frac{V + \omega}{\Delta}\right| \right], \quad (1)$$

where $\delta\epsilon \sim 0.35$ eV is a measure of how much the acceptor level energy, E_a, changes due to the virtual excitation of the core Fe electron, $\Gamma = 0.2$ eV is the width of the acceptor state E_a, $E_{f,s}$ is the position of the Fermi level at the surface of the sample, $\omega = 0.37$ eV (Ref. 35) is the energy splitting of the E and t_2 Fe d-level states, $\Delta \ll \Gamma$ is a cutoff energy, and V is the applied voltage. The value of $\delta\epsilon$ has not been calculated; however, the energy of the exciton is 0.3–0.4 eV and it is plausible that the shift of the electron state E_a will be similar to that energy. This expression for the interfering contribution is valid for regions where the other path is the dominant feature. The path that does not virtually excite a core exciton yields a feature in the dI/dV that is a relatively wide Lorentzian centered around $-E_{f,s}$, and thus it is the dominant feature in the dI/dV for a range of $E_{f,s} \pm 0.2$ eV.

This results in the dI/dV plot of the virtual-exciton-exciting path $\partial I/\partial V$, normalized to the nonexciting path, shown in Fig. 7. In this figure, there are two main trends of interest. The first is the transition of the height of the spike near $eV = -0.37$ eV (corresponding to the energy splitting of the E and T_2 Fe d-level states) from negative to positive. This switch occurs for an increase in $E_{f,s}$. The second trend is the decrease of the dI/dV in voltage regions outside the main feature. This decrease happens for an increase in $E_{f,s}$. The switching of the spike from negative to positive does not substantially affect the topography due to the narrow voltage range of the peak; however, the decrease in the other regions of $\partial I/\partial V$ has a substantial effect because it demonstrates that

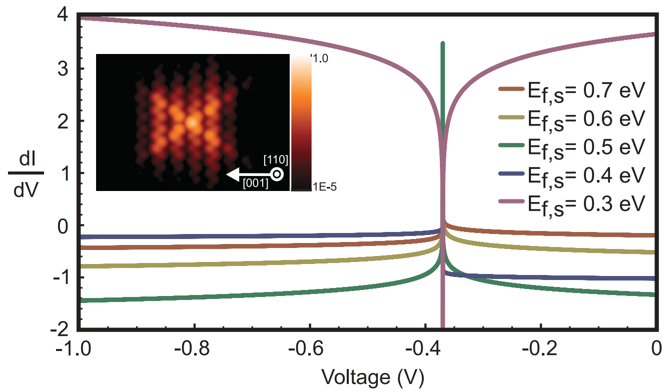

FIG. 7. (Color online) Calculated contribution to dI/dV from the tunneling path that virtually excites a core exciton, in units of the dI/dV from the other tunneling path (that does not), for several potential values of the Fermi energy $E_{f,s}$ near the impurity. Negative values indicate a suppression of the tunneling current. The calculated local density of states of the lowest-energy d state, of E symmetry, using the formalism of Ref. 10 is shown in the inset.

for a large range of negative voltages the Fe image should be dark relative to its surroundings.

We have also calculated the local density of states of the lowest-energy d state, of E symmetry, using the formalism of Ref. 10, but with a tight-binding $spds^*$ Hamiltonian for bulk GaAs, with an on-site potential on the d orbitals of the Fe atom. The potential for the d orbitals is chosen to produce midgap states with energies corresponding to those found experimentally in Ref. 20. The resulting local density of states is shown as an inset in Fig. 7. The large range of voltage for which the calculated $\partial I/\partial V$ is negative, which should produce in topographic maps a dark region (relative to surroundings) which has roughly the size and shape of the E wave function, support an interpretation for the dark anisotropic shapes shown in Fig. 3(b) and indicate that interference effects could be the cause of the decrease in tunneling current for negative applied voltages.

We achieved, via STM, the manipulation of the core state of single Fe impurities in GaAs by controlling the TIBB via the applied voltage. Fe atoms were brought from their isoelectronic state $(Fe^{3+})^0$ into an ionized acceptor state $(Fe^{2+})^-$. The observed local electronic contrast of a single Fe atom was found to change strongly due to different charge states. Finally, a peculiar contrast was observed, in which Fe atoms appear as dark anisotropic features, which we explain by an interference between two elastic tunneling paths.

ACKNOWLEDGMENTS

We acknowledge funding from the European Community's Seventh Framework Programme (PF7/2007-2013) SemiSpin-Net and an AFOSR MURI.

[1] P. M. Koenraad and M. E. Flatté, Nat. Mater. **10**, 91 (2011).
[2] A. Asenov, A. R. Brown, J. H. Davies, S. Kaya, and G. Slavcheva, IEEE Trans. Electron. Dev. **50**, 1837 (2003).
[3] T. Shinada, S. Okamoto, T. Kobayashi, and I. Ohdomari, Nature (London) **437**, 1128 (2005).
[4] M. Fuechsle, J. A. Miwa, S. Mahapatra, H. Ryu, S. Lee, O. Warschkow, L. C. L. Hollenberg, G. Klimeck, and M. Y. Simmons, Nat. Nanotechnol. **7**, 242 (2012).
[5] J. J. Pla, K. Y. Tan, J. P. Dehollain, W. H. Lim, J. J. L. Morton, D. N. Jamieson, A. S. Dzurak, and A. Morello, Nature (London) **489**, 541 (2012).
[6] S. R. Schofield, N. J. Curson, M. Y. Simmons, F. J. Rueß, T. Hallam, L. Oberbeck, and R. G. Clark, Phys. Rev. Lett. **91**, 136104 (2003).
[7] D. Kitchen, A. Richardella, J.-M. Tang, M. E. Flatté, and A. Yazdani, Nature (London) **442**, 436 (2006).
[8] D.-H. Lee and J. A. Gupta, Science **330**, 1807 (2010).
[9] D.-H. Lee and J. A. Gupta, Nano Lett. **11**, 2004 (2011).
[10] J.-M. Tang and M. E. Flatté, Phys. Rev. Lett. **92**, 047201 (2004).
[11] T. O. Strandberg, C. M. Canali, and A. H. MacDonald, Phys. Rev. Lett. **106**, 017202 (2011).
[12] F. Jelezko and J. Wrachtrup, Phys. Status Solidi A **203**, 3207 (2006).
[13] A. M. Yakunin, A. Yu. Silov, P. M. Koenraad, J. H. Wolter, W. Van Roy, J. De Boeck, J.-M. Tang, and M. E. Flatté, Phys. Rev. Lett. **92**, 216806 (2004).
[14] K. Teichmann, M. Wenderoth, S. Loth, R. G. Ulbrich, J. K. Garleff, A. P. Wijnheijmer, and P. M. Koenraad, Phys. Rev. Lett. **101**, 076103 (2008).
[15] A. J. Heinrich, J. A. Gupta, C. P. Lutz, and D. M. Eigler, Science **306**, 466 (2004).
[16] A. M. Yakunin, A. Yu. Silov, P. M. Koenraad, W. Van Roy, J. De Boeck, and J. H. Wolter, Superlattices Microstruct. **34**, 539 (2003).
[17] J. K. Garleff, A. P. Wijnheijmer, C. N. v. d. Enden, and P. M. Koenraad, Phys. Rev. B **84**, 075459 (2011).
[18] S. T. Pantelides (ed.), in *Deep Centers in Semiconductors: A State of the Art Approach*, 2nd ed. (Gordon and Breach, Philadelphia, 1992).
[19] A. Richardella, D. Kitchen, and A. Yazdani, Phys. Rev. B **80**, 045318 (2009).
[20] E. Malguth, A. Hoffmann, and M. R. Phillips, Phys. Status Solidi B **245**, 455 (2008).
[21] K. Pressel, A. Dörnen, G. Rückert, and K. Thonke, Phys. Rev. B **47**, 16267 (1993).
[22] M. Bozkurt, V. A. Grant, J. M. Ulloa, R. P. Campion, C. T. Foxon, E. Marega, G. J. Salamo, and P. M. Koenraad, Appl. Phys. Lett. **96**, 042108 (2010).
[23] J. Bocquel, R. P. Campion, B. L. Gallagher, and P. M. Koenraad (unpublished).
[24] M. C. M. M. van der Wielen, A. J. A. van Roij, and H. van Kempen, Phys. Rev. Lett. **76**, 1075 (1996).
[25] D. Kitchen, A. Richardella, P. Roushan, J.-M. Tang, M. E. Flatté, and A. Yazdani, J. Appl. Phys. **101**, 09G515 (2007).
[26] G. Mahieu, B. Grandidier, D. Deresmes, J. P. Nys, D. Stiévenard, and Ph. Ebert, Phys. Rev. Lett. **94**, 026407 (2005).
[27] C. Çelebi, J. K. Garleff, A. Yu. Silov, A. M. Yakunin, P. M. Koenraad, W. Van Roy, J.-M. Tang, and M. E. Flatté, Phys. Rev. Lett. **104**, 086404 (2010).

[28] J. K. Garleff, C. Çelebi, W. Van Roy, J.-M. Tang, M. E. Flatté, and P. M. Koenraad, Phys. Rev. B **78**, 075313 (2008).
[29] H. Prüser, M. Wenderoth, P. E. Dargel, A. Weismann, R. Peters, T. Pruschke, and R. G. Ulbrich, Nat. Phys. **7**, 203 (2011).
[30] B. C. Stipe, M. A. Rezaei, and W. Ho, Science **280**, 1732 (1998).
[31] B. N. J. Persson and A. Baratoff, Phys. Rev. Lett. **59**, 339 (1987).
[32] L. C. Davis, Phys. Rev. B **2**, 1714 (1970).
[33] A. Bayman, P. K. Hansma, and W. C. Kaska, Phys. Rev. B **24**, 2449 (1981).
[34] A. Baratoff and B. N. J. Persson, J. Vac. Sci. Technol. A **6**, 331 (1988).
[35] B. Clerjaud, J. Phys. C: Solid State Phys. **18**, 3615 (1985).